Inflammatory stimuli recruit cathepsin activity to late endosomal compartments in human dendritic cells

Alfred Lautwein[1,5], Timo Burster[1,5], Ana-Maria Lennon-Duménil[2], Herman S. Overkleeft[3], Ekkehard Weber[4], Hubert Kalbacher[1] and Christoph Driessen[1,5]

[1] Medical and Natural Sciences Research Center, University of Tübingen, Tübingen, Germany
[2] Department of Pathology, Harvard Medical School, Boston, USA
[3] Leiden Institute of Chemistry, Gorleaus Laboratory, Leiden, The Netherlands
[4] Institute of Physiological Chemistry, University of Halle, Halle, Germany
[5] Department of Medicine II, University of Tübingen, Tübingen, Germany

Proteolysis by endocytic cysteine proteases is a central element of the antigen-presentation machinery in dendritic cells (DC). It controls the generation of immunogenic peptides, guides the transit of both MHC class II and MHC-like molecules through the endocytic compartment and converts class II into a peptide-receptive state — features closely linked to DC maturation. Differential activity of endocytic proteases, in particular cathepsins, in subcellular compartments has been implicated as a key regulatory element in controlling this machinery in murine DC. We analyzed the expression and subcellular distribution of the major endocytic cysteine proteases (cathepsins S, B, L and H) along with their major endogenous inhibitor, Cystatin C, in resting and stimulated human DC. Although the majority of cathepsin activity was restricted to lysosomes in resting DC, cathepsins selectively accumulated in late endosomes after LPS-induced stimulation. Surprisingly, expression and distribution of Cystatin C was unaffected by DC maturation. Thus, late endosomes represent a specialized compartment where proteolytic activity is developmentally regulated in DC. This could facilitate the conversion of exogenous protein into MHC class II–peptide complexes.

Received	12/2/02
Revised	22/7/02
Accepted	24/9/02

Key words: Antigen presentation / Dendritic cells / Cathepsins / MHC class II / Endocytic compartments

1 Introduction

DC are highly specialized APC that combine multiple central tasks in both adoptive and innate immunity [1, 2]. The way DC handle MHC class II molecules and antigenic material is key to these functions and requires complex endocytic machinery. Only recently have we started to understand some of this system's basic features, mainly from the murine model [3–9].

In murine DC, the rate-limiting step during processing of the class II invariant chain (Ii) — removal of its N terminus — is performed by the cysteine protease Cathepsin (Cat) S [10], presumably controlled by its endogenous inhibitor Cystatin C. Decreased Cystatin C expression along with changes in its subcellular distribution during maturation resulted in more-efficient sorting of class II to the plasma membrane because of increased CatS activity [5]. Absence of CatS compromises class II transport and affects class II sorting and function [11, 12]. Likewise, the transport of CD1d relies on proper CatS activity [13].

DC use macropinoctosis, mannose-receptors and FcR to concentrate soluble antigen in endocytic compartments [14]. Antigen uptake is down-regulated after exposure to inflammatory stimuli. Efficient conversion of such ingested antigen into class II-bound antigenic peptide is critically dependent on the presence of a maturation stimulus [7, 15]. The underlying mechanism is unknown; however it is believed to be mediated by reducing-enzymes and resident proteases, implicating major changes in the antigen-presentation machinery during DC maturation [7, 15, 16]. In fact, endocytic compartments of DC are structurally reorganized upon stimulation [17].

Cathepsins represent the most abundant family of endocytic proteases [18, 19]. Cathepsins B, D, and S are

[I 22871]

Abbreviations: Cat: Cathepsin **CIIV:** Class II vesicles **ConB:** Concanamycin B **TrfR:** Transferrin-receptor **ER:** Endoplasmic reticulum **MIIC:** MHC class II-enriched compartments **NAG:** N-acetlyl-glucosaminidase

0014-2980/02/1212-3348$17.50+.50/0

known to be expressed in DC [8], and data from cathepsin-deficient mice suggest that CatB and CatS are essential for degradation of exogenous material after FcR-mediated uptake [20].

The endocytic route of APC is a highly dynamic functional unit that comprises a confusing number of morphologically, biochemically or operationally defined subcompartments. Apart from conventional lysosomes and early/late endosomes, MHC class II-enriched compartments (MIIC) and class II vesicles (CIIV) have been described in DC and other types of APC [21, 22]. MIIC are considered the compartment where Ii processing and peptide loading are located. Although still a matter of debate, MIIC most likely match the cell biological criteria of late-endosomal/prelysosomal compartments [23], whereas CIIV appear to be subcompartments specialized in transfer of peptide complexes to the plasma membrane [7]. Given the changes in redox potential and pH along the endocytic route, different endocytic subcompartments might be characterized by distinct patterns of protease activity that could serve key functions in regulating the antigen-processing machinery in DC.

We dissected the subcellular distribution of the major cathepsins in human DC on both the protein and activity level, and demonstrate that cysteine-protease activity is concentrated in late-endosomal/prelysosomal compartments of DC in a maturation-dependent fashion.

2 Results

2.1 Expression of cathepsins and their inhibitors in human DC

Comparing the polypeptide patterns of cathepsins and Cystatin C in whole-cell lysates from resting versus LPS-stimulated DC, we observed little difference (Fig. 1). Only the amount of CatH detectable by immunoblot increased upon DC maturation. The expression of all other cathepsins, including CatS, remained unchanged. CatL was present in DC both in its single-chain form (30 kDa) and its mature 25 kDa two-chain form, whereas it was not detected in monocytes. CatB was more abundant in DC (30 and 33 kDa isoforms as well as a 25 kDa polypeptide), whereas only the 30 kDa form was found in monocytes. In contrast to reports from the murine model, we failed to detect a sizable difference between the amount of Cystatin C expressed in resting versus stimulated human monocyte-derived DC.

To visualize cysteine-protease activity we made use of JPM-565-bio, a bifunctional probe that covalently binds cysteine proteases in an activity-dependent fashion [24].

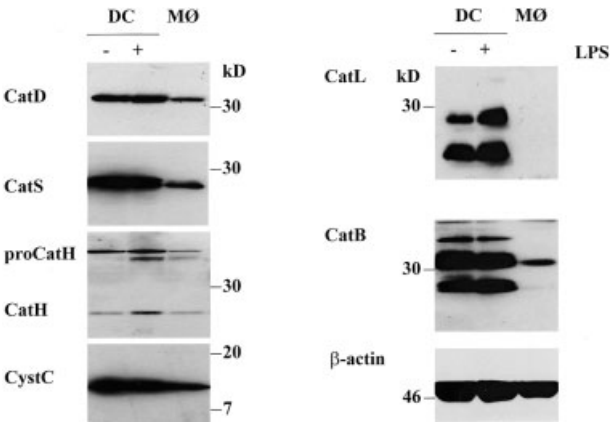

Fig. 1. Expression of cathepsins and Cystatin C in resting versus LPS-stimulated DC and peripheral monocytes (M∅). Lysates (20 μg each) from resting-M∅-derived human DC, DC stimulated with LPS for 24 h or freshly isolated M∅ were resolved by SDS-PAGE and probed for the expression of the cathepsins CatD, CatS, CatH, CatL and CatB, as well as Cystatin C (CystC) and β-actin by immunoblot.

Endocytic fractions of resting DC were incubated with JPM-565-bio, followed by precipitation using streptavidin–sepharose. Samples lacking JPM-565-bio and samples pretreated with its non-biotinylated analog for 30 min prior to labeling served as specificity controls. Precipitates were analyzed by immunoblot with antisera against the respective cathepsins compared with total endocytic fractions to reveal the identity of the active polypeptides targeted (Fig. 2a).

Mature CatS (28 kDa) was detected by direct immunoblot along with its inactive zymogen pro-CatS. In contrast, after active-site-directed labeling followed by precipitation, only mature CatS was visualized, confirming the activity-based nature of labeling. Of the polypeptides visualized for CatB by immunoblot (25, 30, 33 kDa), the 30 and 33 kDa isoforms corresponded to active CatB and were still visualized by CatB antisera after activity-based labeling and precipitation. Most likely, the 25 kDa polypeptide represents an inactive degradation intermediate of the mature enzyme. The activity and identity of CatH and CatL were demonstrated in a similar manner, thus confirming that both the 25 kDa and the 30 kDa isoform of CatL are enzymatically active. Visualization of CatL after active-site-directed targeting and precipitation was only successful when CA074 (1 μM) and LHVS (3 nM) were present throughout the procedure, selectively inhibiting CatB and CatS activity. In the absence of these inhibitors, CatL was not visualized after precipitation (data not shown), suggesting that CatL is destroyed by CatS and CatB in untreated endocytic fractions of DC.

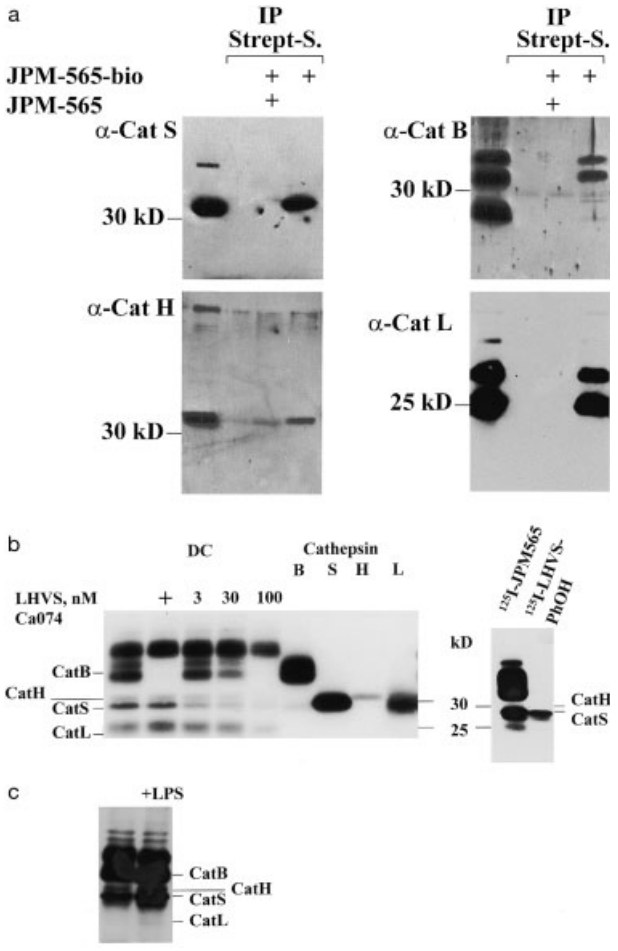

Fig. 2. Visualization of active cathepsins in endocytic fractions. (a) For identification of active cathepsins, endocytic fractions of DC were incubated with JPM-565-bio and the labeled material was retrieved by precipitation (IP) using streptavidin–sepharose beads (Strept-S.). Cathepsins were visualized by immunoblot using appropriate antisera (α-Cat), in comparison with untreated material. Samples preincubated with JPM-565 lacking the biotin moiety and non-labeled samples served as specificity control for labeling and precipitation. (b) Left panel: endocytic fractions from resting DC (10 μg/lane) and purified human cathepsins were labeled with [^{125}I]-JPM-565 and analyzed by SDS-PAGE and autoradiography. Where indicated, the CatS-selective inhibitor LHVS and the CatB inhibitor CA074 were added 30 min prior to labeling. Middle panel: positions of CatB, S, H and L. Right panel: to confirm the identity of CatS, endocytic fractions were labeled with the CatS-selective probe [^{125}I]-LHVS-PhOH in comparison with [^{125}I]-JPM-565. (c) Endocytic fractions of resting or LPS-stimulated DC (20 μg/lane) were labeled with JPM-565-bio, followed by SDS-PAGE and a streptavidin–HRP blot.

Active proteases in DC were then directly visualized by affinity labeling, using either JPM-565-bio or its [^{125}I]-radiolabeled version. For identification, protease-specific inhibitors were added (CA074, specific for CatB, at 1 μM; LHVS is selective for CatS at low nanomolar concentrations, e.g. 3 nM) [8] and the migration pattern of the ploypeptides visualized was compared with that obtained with purified human cathepsins.

The labeling pattern obtained matched that described for murine monocytes and DC using the same probe [20]. A dominant signal at 37 kDa (identified as CatZ in murine monocytes by mass-spectrometry; A-M. Lennon-Duménil, manuscript in preparation) was followed by two polypeptides running at 33 and 35 kDa, respectively. Their labeling was selectively blocked by CA074 and their migration pattern matched that of purified CatB, identifying both as isoforms of active CatB. A faint signal at 31 kDa comigrated with purified CatH and was unaffected by inhibition of CatB or CatS. Since active CatH was precipitated from DC fractions after binding to JPM-565-bio (Fig. 2a), we conclude that this signal corresponded to active CatH, in agreement with murine data [20]. An additional, yet-more-intense signal migrated at 30 kDa. It was unaffected by CA074 but decreased by ~80% after addition of LHVS at 3 nM, identifying it as active CatS. Entirely consistent with that conclusion, purified CatS showed an identical migration pattern and was selectively visualized at this position using the CatS-selective probe [^{125}I]-LHVS-PhOH (Fig. 2b, right panel; [12]). However, the signal obtained at 30 kDa after labeling with [^{125}I]-JPM-565 was not entirely absent after pharmacological elimination of CatS activity (using LHVS at 3 nM). The remaining portion was only blocked at higher concentrations of LHVS, suggesting that this minor portion represented a cysteine protease distinct from CatS. The 30 kDa isoform of CatL that is present in DC and reactive with the probe (Fig. 2a) migrated nearly identically to CatS. The minor portion of the 30 kDa signal could therefore represent this isoform of CatL. Consistent with that interpretation, labeling of this band was completely blocked by 3 nM LHVS in human monocytes lacking CatL (not shown). The mature form of CatL was visualized at 25 kDa, consistent with its reactivity with CatL antisera, and precipitated at its expected molecular weight.

When comparing the JPM-565-bio labeling pattern of resting and LPS-stimulated DC we found no major difference in the active proteases visualized (Fig. 2c). Only CatH showed a slightly increased signal upon maturation, consistent with the results observed at the protein level.

2.2 Separation of endocytic compartments in human DC

To dissect the subcellular distribution of endocytic proteases and their inhibitors, we employed a subcellular-fractionation protocol that allows separation of the major subcellular compartments of class II transport [12, 18, 25, 26]. Postnuclear supernatants of homogenized DC were separated on a 27% Percoll gradient, yielding a lysosomal fraction [peak A: high density; LAMP-1$^+$, and N-acetyl-glucosaminidase (NAG)$^+$], together with unresolved material at the top of the gradient (Fig. 3a). This low-density fraction was subjected to a 10% Percoll gradient where a pre-lysosomal/late-endosomal fraction [peak B: intermediate density; LAMP-1$^+$, NAG$^+$, transferrin-receptor (TrfR)$^-$] was separated from the remainder [peak C: low density, plasma membrane, Golgi, endoplasmic reticulum (ER), early endosomes; NAG$^+$, TrfR$^+$, LAMP-1$^-$]. The distribution of endocytic markers was in good agreement with previous data published for murine DC and murine monocytes. No significant difference was observed between resting and LPS-stimulated DC.

When we examined the steady-state distribution of MHC II in resting versus LPS-stimulated DC, the result was entirely consistent with earlier morphological, phenotypical and biochemical data for both human and murine DC (Fig. 3b). In resting DC, only small amounts of class II sedimented with the plasma membrane (peak C), whereas the majority cofractionated with LAMP-1$^+$ endocytic compartments (peaks A and B). Upon stimulation with LPS, a substantial increase of class II in the low-density fractions, in essence representing plasma membrane, was observed.

2.3 Subcellular distribution of proteolytic activity in DC

We used JPM-565-bio to map the subcellular distribution of protease activity. Endocytic organelles were recovered from subcellular fractions of resting or LPS-stimulated DC by ultracentrifugation and lysed at pH 5 under reducing conditions before labeling and visualization (Fig. 4).

As in total endocytic compartments, the major polypeptides labeled were cathepsins S, B, and H. CatL was barely visible, most likely due to its protease lability. In resting DC, the majority of cysteine-protease activity was visualized in lysosomes (fraction A) with significant activity also present in late-endosomal/prelysosomal fractions (B). Little activity of CatB and CatS was detected in fraction C. In contrast, LPS-stimulated DC contained

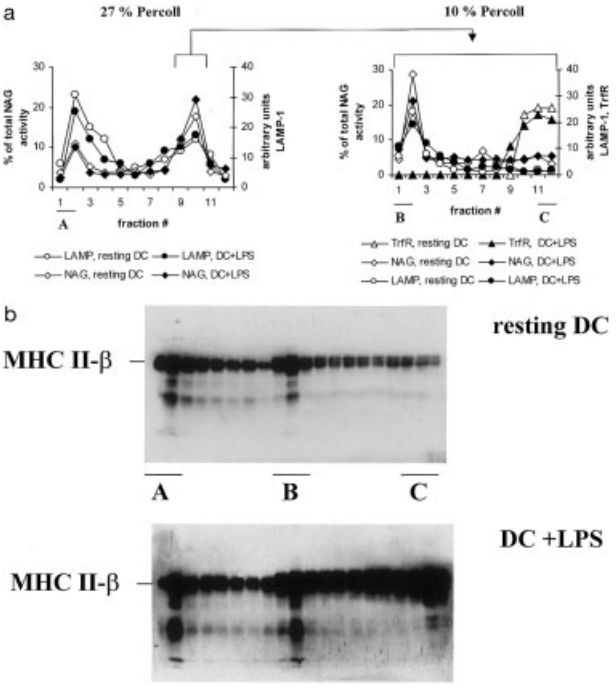

Fig. 3. (a) Distribution of endocytic marker proteins in subcellular fractions derived from resting or LPS-stimulated human DC. Monocyte-derived human DC were subjected to subcellular fractionation with (+LPS) and without (resting DC) prior stimulation for 24 h. Postnuclear supernatants were resolved on consecutive Percoll gradients as described, yielding three peaks of NAG activity (A, B, C). Subcellular organelles were retrieved by ultracentrifugation and assayed for the distribution of the late endocytic marker LAMP-1 and the early-endosomal/plasma-membrane marker TrfR by Western blot followed by densitometry-based semiquantitative assessment of the respective signals. Results from each fraction are expressed as % of the total signal retrieved in the respective gradient. A, B, and C represent the major activity peaks referred to as lysosomes (A), late-endosomes/prelysosomes (B) and early-endosomes/plasma-membrane (C) in good agreement with the published characteristics of the method [12]. (b) Subcellular distribution of MHC class II in resting versus LPS-stimulated DC. Subcellular fractions obtained as described from resting versus LPS-stimulated DC (Fig 3a) were analyzed for the distribution of the MHC class II β-chain by Western blot.

their maximum total cathepsin activity in the late-endosomal/prelysosomal compartment where active CatS and CatB were concentrated whereas lysosomal protease activity was less prominent. In particular, CatS activity was strongly diminished in lysosomes. Some active CatB was also found in the early-endosomal/plasma-membrane fraction C from mature DC, in contrast to resting cells.

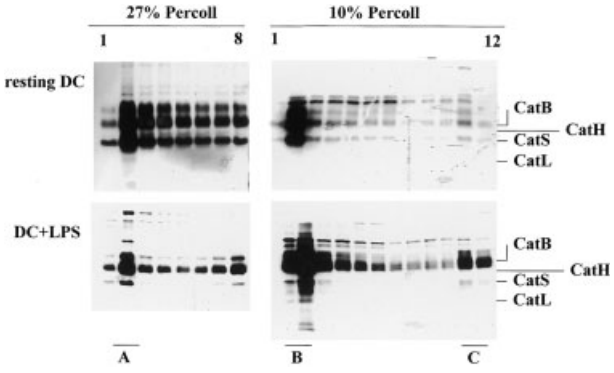

Fig. 4. Subcellular distribution of active cysteine-proteases in resting versus stimulated DC. Subcellular fractions from resting or LPS-stimulated DC were analysed for the distribution of active cysteine-proteases using JPM-565-bio. One half of each DC-preparation from six individuals was stimulated by LPS during the last 24 h of culture, while the other half remained untouched. DC were harvested and pooled (resting versus LPS-stimulated) prior to preparation of post-nuclear supernatants and fractionation. Endocytic organelles were retrieved by ultracentrifugation, lysed at pH 5.0 under reducing conditions and subjected to the labeling procedure. Active proteases were visualized by streptavidin-HRP after resolution by SDS-PAGE and transfer on PVDF membranes.

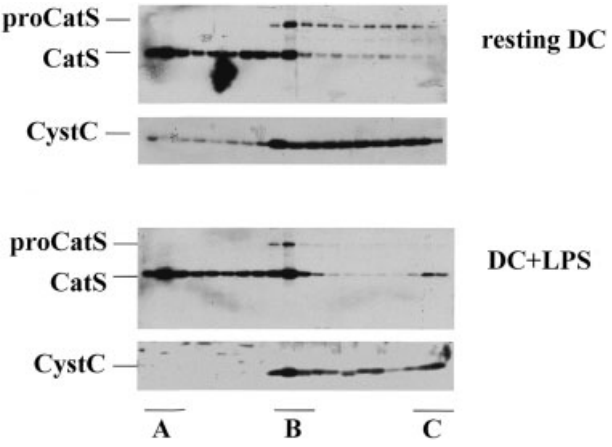

Fig. 5. Subcellular distribution of CatS and Cystatin C (CystC) in resting versus LPS-stimulated DC. Subcellular fractions from resting and LPS-stimulated DC (Fig. 3, 4) were probed for the distribution of CatS and CystC by immunoblot.

2.4 Cystatin C colocalizes with active cathepsins in late endosomes

Is the differential distribution of CatS activity in resting versus activated human DC mainly due to differential transport of CatS or is it linked to changes in transport and/or expression of endogenous inactivating factors such as Cystatin C? To this end, we performed immunoblot-type experiments with subcellular fractions from resting and activated DC (Fig. 5).

In resting DC, CatS reached late-endosomal/prelysosomal compartments in its pro-form. There, pro-CatS colocalized with CatS, implicating proteolytic conversion of pro-CatS into its active form at this location and confirming the late-endosomal/prelysosomal nature of peak B. Exclusively mature CatS was found in the lyosomal compartment whereas pro-CatS was absent. Upon DC maturation, this pattern remained essentially intact, although small amounts of mature CatS were also found in low-density fractions. Regarding the bulk of mature CatS, the differential distribution of CatS activity in resting versus mature DC was not due to gross changes in the subcellular distribution of CatS protein.

Strikingly, the distribution pattern of Cystatin C was distinct from that of CatS: Cystatin C was virtually absent from lysosomal compartments but was found in the peaks B and C, consistent with its localization in late-endosomes/prelysosomes, as well as in the Golgi/ER/early-endosomal compartment, the latter in large agreement with typical characteristics of a secretory protein. Of note, and in contrast to earlier observations from murine DC [5], we found an identical distribution pattern for Cystatin C in resting versus LPS-stimulated human DC. Thus, differential activity of CatS in late-endosomes/prelysosomes of resting versus mature human DC is not linked to alterations in the expression or distribution of Cystatin C.

2.5 Visualization of cysteine-protease activity in non-disrupted endocytic compartments

Endocytic pH, redox-potential and structural changes induced in the endocytic compartment of DC upon maturation are destroyed once the membrane integrity is disrupted prior to analysis. The hydrophobic nature of the active-site-directed probe CBz-[^{125}I]Tyr-Ala-CN_2, which visualizes active CatB and CatS in DC [8], allows targeting of proteases in intact endocytic compartments.

When CBz-[^{125}I]Tyr-Ala-CN_2 was incubated with intact DC in the presence/absence of LHVS (3 nM) or leupeptin (1 μM), respectively, the autoradiograph of the lysates after resolution by SDS-PAGE confirmed both the identity of the signals retrieved and the specificity of labeling (Fig. 6a). To assess the intracellular distribution of active cathepsins during DC-maturation, DC were treated with LPS for 0, 3 or 24 h and subjected to subcellular fraction-

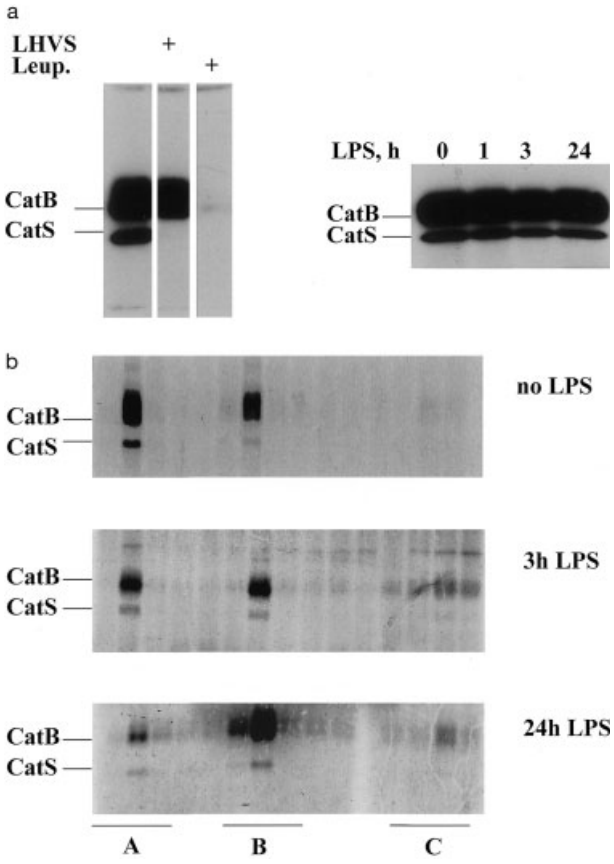

Fig. 6. Visualization of active cathepsins in intact endocytic organelles of resting versus stimulated DC using CBz-[^{125}I]Tyr-Ala-CN. (a) Left panel: intact DC were either left untreated or preincubated with the CatS-inhibitor LHVS or the cysteine-protease inhibitor leupeptin (Leup.), respectively, prior to labeling with CBz-[^{125}I]Tyr-Ala-CN. After lysis in heated sample-buffer, active cysteine-proteases were visualized by SDS-PAGE and autoradiography. Right panel: treatment of DC with LPS for the times indicated prior to active-site-directed labeling using CBz-[^{125}I]Tyr-Ala-CN. (b) DC were stimulated with LPS for 0, 3, and 24 h, respectively, and subjected to subcellular fractionation. After retrieving the endocytic organelles from the subcellular fractions by ultracentrifugation at each time-point, endocytic organelles were exposed to CBz-[^{125}I]Tyr-Ala-CN for 30 min without prior disruption by detergent. Lysis was achieved by addition of boiling SDS-sample-buffer after the labeling reaction, followed by SDS-PAGE and autoradiography.

ation. Endocytic organelles were immediately recovered by ultracentrifugation and labeled with CBz-[^{125}I]Tyr-Ala-CN_2, leaving the endocytic organelles intact. Lysis was performed in denaturing SDS-sample-buffer at 95°C, preventing post-lysis labeling of released proteases, prior to SDS-PAGE and autoradiography (Fig. 6b). In resting DC, the majority of CatS and CatB activity was detected in lysosomal compartments. Significantly less CatS and B was active in fractions corresponding to late-endosomes/prelysosomes whereas both activities were absent from peak C, consistent with our data using JPM565 and at the protein level, respectively. After 3 h of LPS-treatment, a nearly equal distribution of the activity of both proteases was observed between lysosomes and late-endosomes/prelysosomes, with little activity in peak C. In particular, active CatS, which was barely detectable in late endosomal fractions under resting conditions but strongly present in lysosomes, had significantly changed its subcellular distribution. Already after 3 h of LPS challenge it was present at similar levels in lysosomal and late endosomal compartments. After 24 h of LPS-induced DC-maturation, CatS and CatB were most prominent in late-endosomes/prelysosomes with considerably less activity in lysosomes. Thus, DC-maturation controls the intracellular distribution of protease activity in DC and concentrates CatB and CatS activity in late endosomal compartments.

2.6 DC maturation promotes the intracellular degradation of protein taken up via FcγII receptor

To demonstrate that the cathepsins concentrated in late endosomes of human DC upon maturation are functional, we assessed the kinetics of degradation of a complex protein after its uptake via FcγRII. We made use of an established model that tracks the degradation of radiolabeled [^{125}I]-anti-mouse $F(ab')_2$ fragments directed to late endosomes via FcγRII [8, 20]. FcγRII delivers polyvalent ligands to late endosomes for class II-mediated antigen presentation [27]. To localize the intracellular site of delivery and degradation of the model antigen, we incubated resting DC with a murine anti-FcγRII antibody on ice for 30 min, followed by washes at 4°C and incubation with radiolabeled sheep anti-mouse [^{125}I]-$F(ab')_2$ fragments. After repeated washing, cells were shifted to 37°C for 1 h to allow internalization of the radiolabeled complex, before exposing them to pH 3 for 5 min, which disrupts antigen–antibody interactions at the cell surface and releases non-internalized material into the supernatant, as demonstrated previously [20]. After washing, cells were fractionated yielding the peak fractions A, B, and C. Analysis of the distribution of radiolabeled polypeptides by SDS-PAGE and autoradiography revealed that indeed the majority of [^{125}I]-$F(ab')_2$ fragments had been delivered to compartment B (late endosomes), where their degradation occurred (Fig. 7a). We observed a prominent signal (26 kDa) representing intact radiolabeled $F(ab')_2$ fragments of heavy and light chains, respectively, followed by a less abundant signal (23 kDa), that represents an intermediate of intracellular degradation whose generation relies on CatB activity.

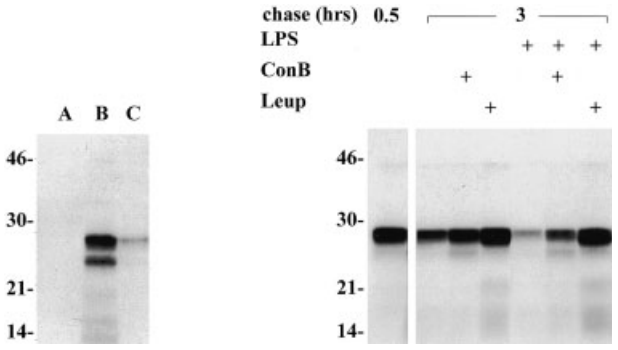

Fig. 7. Intracellular degradation of the model antigen [^{125}I]-F(ab')$_2$ in resting versus LPS-stimulated DC. (a) DC were loaded with [^{125}I]-F(ab')$_2$ fragments via FcγRII as described, chased for 1 h and subjected to subcellular fractionation. Distribution of the radiolabeled polypeptides between the pooled peak fractions A–C (10% by volume of each peak) was visualized by SDS-PAGE and autoradiograhy. (b) The kinetics of the intracellular degradation of ^{125}I-F(ab')$_2$ were compared between resting DC and DC undergoing LPS challenge. After internalization of [^{125}I]-F(ab')$_2$ fragments via FcγR (0.5 h), cells were chased in the presence/absence of LPS for 3 h, with or without addition of leupeptin (Leup) or ConB, followed by SDS-PAGE and autoradiography.

Additional, poorly resolved intermediates were visualized at 21 and 14 kDa, respectively, essentially as reported previously [20]. Compartment C (early endosomes and plasma membrane) contained only the intact 26-kDa-radiolabeled species, consistent with little degradation at this location, whereas no radioactive signal was retrieved from the lysosomal compartment A. Thus degradation of the FcγRII-bound [^{125}I]-F(ab')$_2$ model antigen is observed in late endosomes in human DC.

CatS and CatB are the rate-limiting enzymes in the intracellular turnover of [^{125}I]-F(ab')$_2$ fragments in this model [8, 20]. If the accumulation of CatS and CatB in late endosomes induced upon LPS-mediated stimulation of DC (Fig. 5, 6) is functionally relevant, this should affect the intracellular degradation of [^{125}I]-F(ab')$_2$. DC were therefore incubated with the mouse anti-FcγRII plus anti-mouse-[^{125}I]-F(ab')$_2$ reagents under the conditions described and shifted to 37°C for 30 min to allow the FcγRII-mediated internalization of the complex (pulse), followed by pH 3 treatment for 5 min as before. During the subsequent chase (3 h at 37°C), LPS was added to one half of the sample, in either the presence or absence of inhibitors of cysteine proteases (leupeptin, 1 μM) or Concanamycin B [(ConB), 20 nM, an antagonist of endocytic acidification and transport] [18]. Samples were lysed in SDS under reducing conditions and analyzed by SDS-PAGE and autoradiography (Fig. 7b). Each lane represents an equal number of cells.

After the pulse we observed exclusively the 26 kDa species representing intact F(ab')$_2$ fragments. After 3 h of chase in the absence of LPS, the intensity of this signal was reduced, indicating intracellular degradation. This was partially antagonized by ConB and blocked by elimination of cysteine-protease activity (leupeptin), confirming that cysteine proteases mediate the degradation of F(ab')$_2$ fragments in human DC in this system.

Samples chased in the presence of LPS showed a significantly higher turnover of radiolabeled F(ab')$_2$ fragments during the chase, compared with non-stimulated controls. Again, addition of ConB partially antagonized this effect, whereas treatment with leupeptin blocked F(ab')$_2$ degradation. Thus, the LPS-induced maturation of DC led to a significantly more efficient degradation of the F(ab')$_2$ complexes previously delivered to late endosomes within 3 h after administration of the maturation stimulus. This effect is mediated by the activity of endocytic cysteine-proteases and can be blocked by addition of leupeptin. We suggest that it functionally reflects the accumulation of active cathepsins, in particular CatS and CatB, in late endosomes of LPS-stimulated human DC.

3 Discussion

DC control MHC class II-mediated antigen-presentation via maturation-induced changes in both structure and function of their endocytic compartment. Endocytic proteases have been implicated as a central regulatory element of this machinery [4, 5, 8, 17]. We here present a first analysis of the distribution of protease activity in the endocytic compartment of human DC. Cathepsins S, L, B, H are active in human DC. Although they are located primarily in lysosomes in resting DC, their activity is concentrated in late endosomes after administration of a maturation signal, coincident with the accumulation of class II on the cell surface and accelerated late-endosomal degradation of a model antigen whose destruction is dominated by CatS and CatB. This intracellular redistribution of cathepsin activity is detectable after 3 h of maturation and reaches a maximum after 24 h.

Redistribution of cathepsins was not accompanied by changes in the expression profile or subcellular distribution of CatS polypeptides. It is therefore likely to depend on the conditions that functionally regulate endocytic protease activity, most likely local pH and the availability of endogenous protease activators or inhibitors. When endocytic compartments were left intact during active-site-directed labeling, the intracellular redistribution of proteolytic activity upon DC maturation was most obvi-

ous. This argues that factors linked to membrane integrity are important for the regulation of protease function. Changes in endocytic pH and/or the microarchitecture of endocytic compartments, which both accompany DC maturation, might be part of the regulatory mechanism [8]. Morphological changes in the endocytic compartments could regulate the access of endocytic proteases to endogenous inhibitors/activators, creating new functional compartments, in analogy to what has been suggested for the access of class II to HLA-DM [17]. Alternatively, a decrease in endocytic pH upon DC maturation could dislodge the inhibitory propiece from the active site of cysteine proteases in late-endosomal/prelysosomal compartments [28], leading to their activation further upstream in the endocytic pathway. Indeed, we found pro-CatS predominantly in the late-endosomal/prelysosomal compartment. Also consistent with this view is the notion that inhibition of endocytic acidification impairs the activity of both CatS and CatB [8], although purified CatS is functional at neutral pH.

A significant shift of protease activity, in particular CatS and CatB, toward late-endosomes/prelysosomes was still visualized when the regulatory influence of endocytic pH and endogenous reducing conditions was eliminated. This implies that endogenous activators/inhibitors of protease activity that are independent from these factors are also involved in the regulating process, not unlike the view of Pierre et al., who suggested that differential distribution and activity of Cystatin C is a hallmark of DC maturation [5]. According to our data, Cystatin C colocalized with active cathepsins in late endosomes, not in lysosomes, of human DC. It is therefore likely to selectively inhibit cathepsin activity in late-endosomes/MIIC, which might ensure controlled processing of both antigen and Ii under steady-state conditions, while preventing excessive proteolysis of antigenic epitopes and other functionally important molecules, in contrast to lysosomes. However, neither expression nor subcellular distribution of Cystatin C changed upon DC maturation, although late endosomal CatS activity was up-regulated and a significantly increased fraction of class II was targeted to the cell surface. Differential expression or subcellular distribution of Cystatin C is therefore unlikely to control either the maturation-induced increase of late endosomal cathepsin activity or the delivery of class II to the plasma membrane in LPS-stimulated human DC. Given the high activity of proteases in DC, however, it is not unlikely that as-yet-unidentified protease inhibitors are present in their endocytic compartment. Differential subcellular distribution and/or activity of these inhibitors might be better candidates to explain the effects observed.

What is the possible function of cathepsin activity that accumulates in late endosomes of DC challenged with LPS? Two parallel studies demonstrated that hen egg lysozyme (HEL) internalized by resting DC was not converted into class II-bound HEL peptide within up to 60 h of chase unless LPS was added. LPS, however, triggered the intracellular appearance of such material within 4 h, reaching a maximum at 9 h, followed by subsequent transport to the plasma membrane where it accumulated at ~18 h. Thus, resting DC do not efficiently convert antigenic protein into class II-bound peptide unless a maturation signal is supplied, but store antigenic material in late endocytic compartments [7, 15]. The underlying mechanism is unknown; increased CatS activity due to down-regulation of Cystatin C, changes in the function of other endocytic proteases, as well as alterations in the acidity of the endocytic system during DC maturation are the models discussed. We here demonstrate such increased activity of CatS in late endosomal compartments of human DC within 3 h after addition of the maturation stimulus (Fig. 6b), that further increases until 24 h. In agreement with this, the proteolysis of an internalized model antigen whose breakdown relies on CatB and CatS in late endosomal compartments [20], is accelerated after addition of LPS. Thus, CatS and CatB increase their local activity in late endosomes within hours after addition of the maturation stimulus, leading to more-efficient local proteolysis. This might enable the loading of antigenic material stored in this compartment either by facilitating the local conversion of Iip10 into CLIP or by allowing the breakdown of relatively stable antigenic processing intermediates into immunogenic peptides suitable for class II binding. Alternatively, it might trigger the morphological reorganization and formation of novel endocytic compartments like CIIV [7, 17] by limited proteolysis of regulatory proteins that govern subcellular transport.

4 Materials and methods

4.1 Cells, antibodies and proteases

Human DC were generated from adherent monocytes using IL-4 and GM-CSF, essentially as described previously [16], and matured with 1 μg/ml LPS (Sigma) for the last 24 h of culture. FACS analysis revealed a 70–85% pure DC population that up-regulated class II, CD40, B7.1 and B7.2 as well as CD83 upon stimulation. The majority of the remaining cells were T cells, with few B lymphocytes (less than 10% of total). Peripheral blood monocytes were isolated from PBMC using a Percoll gradient, resulting in a population enriched for monocytes (70–80% of cells were class-II$^+$, CD14$^+$, CD1a$^-$).

Anti-cathepsin antisera were generated by E. Weber against recombinant cathepsins; anti-TrfR and anti-LAMP-1 antibodies were purchased from Pharmingen; the polyclonal

serum against class II β-chain was obtained from H. Ploegh, Boston; the rabbit anti-Cystatin-C antiserum was from Upstate Biotechnologies. Purified human cathepsins were a gift from R. Riese and H. Chapman, Boston.

4.2 Subcellular fractionation

Subcellular fractions were prepared and characterized exactly as described previously [12, 18, 25, 26]. After fractionation, organelles were recovered by centrifugation at 100,000×g for 10 min. For depletion of cytosol from endocytic organelles (referred to as "endocytic fractions" in the text), postnuclear supernatants were sedimented (100,000×g for 2 min) as described previously [29].

4.3 Western blot

Cells and fractions were lysed in NP-40 lysis buffer, pH 7 (50 mM sodium acetate, 5 mM $MgCl_2$, 0.5% NP-40) and were resolved by 12.5% SDS-PAGE, transferred to PVDF membranes (Millipore), blocked, and probed with appropriate dilutions of the respective primary antibody, followed by a secondary anti-rabbit IgG antibody coupled with peroxidase (Southern Biotech). An ECL detection kit (Amersham Pharmacia) was used to visualized the Ab-reactive proteins.

4.4 Active-site-directed labeling

JPM-565, JPM-565-bio and LHVS-PhOH were synthesized essentially as described for the non-biotinylated version of the compounds [30]; the biotin moiety was attached as described for LVHS-bio [26]. CBz-Tyr-Ala-CN_2 was a kind gift from H. Ploegh, Boston. Radioiodination was achieved using the iodogen method (Pierce) according to the manufacturer's advice using a disposable C18 matrix (Waters) for purification [12]. Enriched subcellular fractions were lysed in NP-40 lysis buffer, pH 5 (50 mM sodium acetate, 5 mM $MgCl_2$, 0.5% NP-40) and analyzed for protein concentration using the Bio-Rad Bradford reagent. Lysates were incubated with 1 mM JPM565–biotin/[^{125}I]-JPM-565/[^{125}I]-LHVS-PhOH for 1 h at 37°C. For selective inhibition of proteases, appropriate inhibitors were added 30 min prior to labeling. Reactions were terminated by addition of SDS reducing sample buffer and immediate boiling. Samples were resolved by 12.5% SDS-PAGE gels and either directly analyzed by autoradiography or transferred to PVDF membranes, followed by visualization using streptavidin–HRP solution and the ECL-detection kit (Amersham). Intact cells (1×10^6 DC) or intact endocytic organelles retrieved by ultracentrifugation from subcellular fractions, respectively, were labeled with CBz-[^{125}I]-Tyr-Ala-CN_2 in serum-free medium at 37°C for 30 min, with or without prior inhibition of cysteine proteases by LHVS or leupeptin. Samples were washed twice with ice-cold PBS and lysed by addition of 2×SDS sample buffer immediately followed by boiling. After resolution by SDS-PAGE, active proteases were visualized by autoradiography.

4.5 Precipitation of active proteases

Endocytic fractions of resting DC were precleared with streptavidin–sepharose beads overnight before being split into three equal portions in lysis buffer at pH 5. Portion 1 remained untouched, portion 2 was preincubated with non-biotinylated JPM-565 (30 min at 37°C). Samples 2 and 3 were then incubated with JPM-565-bio as described. Excess label was removed using a PD10 column (Pharmacia) and labeled polypeptides were recovered using streptavidin–sepharose beads (Pharmacia). After excessive washing, samples were resolved on SDS-PAGE side by side with untreated endocytic fractions and further analyzed by western blot using anti-cathepsin antisera.

4.6 Intracellular degradation of [^{125}I]-F(ab')$_2$ fragments

Analysis of the intracellular degradation of the model antigen [^{125}I]-F(ab')$_2$ was performed exactly as recently described [20], with the only modification that sheep anti-mouse [^{125}I]-F(ab')$_2$ fragments (Amersham) and a murine anti-FcγIIR-antibody (IV.3, Medatrex) were used for the procedure.

Acknowledgement: This work was supported by the Deutsche Forschungsgemeinschaft (DR378.2–1, SFB 510).

References

1 **Rescigno, M. and Borrow, P.,** The host-pathogen interaction: new themes from dendritic cell biology. *Cell* 2001. **106:** 267–270.

2 **Lanzavecchia, A. and Sallusto, F.,** Regulation of T cell immunity by dendritic cells. *Cell* 2001. **106:** 263–266.

3 **Villadangos, J. A. and Ploegh, H. L.,** Proteolysis in MHC class II antigen presentation: who's in charge? *Immunity* 2000. **12:** 233–239.

4 **Pierre, P., Turley, S. J., Gatti, E., Hull, M., Meltzer, J., Mirza, A., Inaba, K., Steinman, R. M. and Mellman, I.,** Developmental regulation of MHC class II transport in mouse dendritic cells. *Nature* 1997. **388:** 787–792.

5 **Pierre, P. and Mellman, I.,** Developmental regulation of invariant chain proteolysis controls MHC class II trafficking in mouse dendritic cells. *Cell* 1998. **93:** 1135–1145.

6 **Mellman, I. and Steinman, R. M.,** Dendritic cells: specialized and regulated antigen processing machines. *Cell* 2001. **106:** 255–258.

7 **Turley, S. J., Inaba, K., Garrett, W. S., Ebersold, M., Unternaehrer, J., Steinman, R. M. and Mellman, I.,** Transport of peptide-MHC class II complexes in developing dendritic cells. *Science* 2000. **288:** 522–527.

8 **Fiebiger, E., Meraner, P., Weber, E., Fang, I. F., Stingl, G., Ploegh, H. and Maurer, D.,** Cytokines regulate proteolysis in major histocompatibility complex class II-dependent antigen presentation by dendritic cells. *J. Exp. Med.* 2001. **193:** 881–892.

9 **Villadangos, J. A., Cardoso, M., Steptoe, R. J., van Berkel, D., Pooley, J., Carbone, F. R. and Shortman, K.,** MHC class II expression is regulated in dendritic cells independently of invariant chain degradation. *Immunity* 2001. **14:** 739–749.

10 **Villadangos, J. A., Riese, R. J., Peters, C., Chapman, H. A. and Ploegh, H. L.,** Degradation of mouse invariant chain: roles of cathepsins S and D and the influence of major histocompatibility complex polymorphism. *J. Exp. Med.* 1997. **186:** 549–560.

11 **Shi, G. P., Villadangos, J. A., Dranoff, G., Small, C., Gu, L., Haley, K. J., Riese, R., Ploegh, H. L. and Chapman, H. A.,** Cathepsin S required for normal MHC class II peptide loading and germinal center development. *Immunity* 1999. **10:** 197–206.

12 **Driessen, C., Bryant, R. A., Lennon-Dumenil, A. M., Villadangos, J. A., Bryant, P. W., Shi, G. P., Chapman, H. A. and Ploegh, H. L.,** Cathepsin S controls the trafficking and maturation of MHC class II molecules in dendritic cells. *J. Cell Biol.* 1999. **147:** 775–790.

13 **Riese, R. J., Shi, G. P., Villadangos, J., Stetson, D., Driessen, C., Lennon-Dumenil, A. M., Chu, C. L., Naumov, Y., Behar, S. M., Ploegh, H., Locksley, R. and Chapman, H. A.,** Regulation of CD1 function and NK1.1(+) T cell selection and maturation by Cathepsin S. *Immunity* 2001. **15:** 909–919.

14 **Sallusto, F., Cella, M., Danieli, C. and Lanzavecchia, A.,** Dendritic cells use macropinocytosis and the mannose receptor to concentrate macromolecules in the major histocompatibility complex class II compartment: downregulation by cytokines and bacterial products. *J. Exp. Med.* 1995. **182:** 389–400.

15 **Inaba, K., Turley, S., Iyoda, T., Yamaide, F., Shimoyama, S., Reis e Sousa, C., Germain, R. N., Mellman, I. and Steinman, R. M.,** The formation of immunogenic major histocompatibility complex class II-peptide ligands in lysosomal compartments of dendritic cells is regulated by inflammatory stimuli. *J. Exp. Med.* 2000. **191:** 927–936.

16 **Cella, M., Engering, A., Pinet, V., Pieters, J. and Lanzavecchia, A.,** Inflammatory stimuli induce accumulation of MHC class II complexes on dendritic cells. *Nature* 1997. **388:** 782–787.

17 **Kleijmeer, M., Ramm, G., Schuurhuis, D., Griffith, J., Rescigno, M., Ricciardi-Castagnoli, P., Rudensky, A. Y., Ossendorp, F., Melief, C. J., Stoorvogel, W. and Geuze, H. J.,** Reorganization of multivesicular bodies regulates MHC class II antigen presentation by dendritic cells. *J. Cell Biol.* 2001. **155:** 53–63.

18 **Villadangos, J. A., Driessen, C., Shi, G. P., Chapman, H. A. and Ploegh, H. L.,** Early endosomal maturation of MHC class II molecules independently of cysteine proteases and H-2DM. *EMBO J.* 2000. **19:** 882–891.

19 **Chapman, H. A.,** Endosomal proteolysis and MHC class II function. *Curr. Opin. Immunol.* 1998. **10:** 93–102.

20 **Driessen, C., Lennon-Dumenil, A. M. and Ploegh, H. L.,** Individual cathepsins degrade immune complexes internalized by antigen-presenting cells via Fc gamma receptors. *Eur. J. Immunol.* 2001. **31:** 1592–1601.

21 **Amigorena, S., Drake, J. R., Webster, P. and Mellman, I.,** Transient accumulation of new class II MHC molecules in a novel endocytic compartment in B lymphocytes. *Nature* 1994. **369:** 113–120.

22 **Peters, P. J., Raposo, G., Neefjes, J. J., Oorschot, V., Leijendekker, R. L., Geuze, H. J. and Ploegh, H. L.,** Major histocompatibility complex class II compartments in human B lymphoblastoid cells are distinct from early endosomes. *J. Exp. Med.* 1995. **182:** 325–334.

23 **Kleijmeer, M. J., Morkowski, S., Griffith, J. M., Rudensky, A. Y. and Geuze, H. J.,** Major histocompatibility complex class II compartments in human and mouse B lymphoblasts represent conventional endocytic compartments. *J. Cell Biol.* 1997. **139:** 639–649.

24 **Bogyo, M., Verhelst, S., Bellingard-Dubouchaud, V., Toba, S. and Greenbaum, D.,** Selective targeting of lysosomal cysteine proteases with radiolabeled electrophilic substrate analogs. *Chem. Biol.* 2000. **7:** 27–38.

25 **Castellino, F. and Germain, R. N.,** Extensive trafficking of MHC class II-invariant chain complexes in the endocytic pathway and appearance of peptide-loaded class II in multiple compartments. *Immunity* 1995. **2:** 73–88.

26 **Lennon-Dumenil, A. M., Roberts, R. A., Valentijn, K., Driessen, C., Overkleeft, H. S., Erickson, A., Peters, P. J., Bikoff, E., Ploegh, H. L. and Wolf Bryant, P.,** The p41 isoform of invariant chain is a chaperone for cathepsin L. *EMBO J* 2001. **20:** 4055–4064.

27 **Mellman, I. and Plutner, H.,** Internalization and degradation of macrophage Fc receptors bound to polyvalent immune complexes. *J. Cell Biol.* 1984. **98:** 1170–1177.

28 **Wiederanders, B.,** The function of propeptide domains of cysteine proteinases. *Adv. Exp. Med. Biol.* 2000. **477:** 261–270.

29 **Schroter, C. J., Braun, M., Englert, J., Beck, H., Schmid, H. and Kalbacher, H.,** A rapid method to separate endosomes from lysosomal contents using differential centrifugation and hypotonic lysis of lysosomes. *J. Immunol. Methods* 1999. **227:** 161–168.

30 **Shi, G. P., Bryant, R. A., Riese, R., Verhelst, S., Driessen, C., Li, Z., Bromme, D., Ploegh, H. L. and Chapman, H. A.,** Role for cathepsin F in invariant chain processing and major histocompatibility complex class II peptide loading by macrophages. *J. Exp. Med.* 2000. **191:** 1177–1186.

Correspondence: Christoph Driessen, MNF Universität Tübingen, Ob dem Himmelreich 7, 72074 Tübingen, Germany
Fax: +49–7071-87815
e-mail: christoph.driessen@uni-tuebingen.de